

Spectroscopy of thulium and holmium heavily doped tellurite glasses

Original

Spectroscopy of thulium and holmium heavily doped tellurite glasses / Gebavi, H.; Milanese, Daniel; Balda, R.; Taccheo, S.; Fernandez, J.; Lousteau, Joris; Ferraris, Monica. - In: JOURNAL OF LUMINESCENCE. - ISSN 0022-2313. - STAMPA. - 132:(2012), pp. 270-276. [10.1016/j.jlumin.2011.08.042]

Availability:

This version is available at: 11583/2497360 since:

Publisher:

Elsevier B.V.

Published

DOI:10.1016/j.jlumin.2011.08.042

Terms of use:

This article is made available under terms and conditions as specified in the corresponding bibliographic description in the repository

Publisher copyright

(Article begins on next page)

Spectroscopy of thulium and holmium heavily doped tellurite glasses

H. Gebavi^{1,*}, D. Milanese¹, R. Balda², S. Taccheo³, J. Fernandez², J. Lousteau¹, M. Ferraris¹

This is the author post-print version of an article published on *Journal of Luminescence*, Vol. 132, pp. 270-276, 2012 (ISSN 0022-2313).

The final publication is available at

<http://dx.doi.org/10.1016/j.jlumin.2011.08.042>

This version does not contain journal formatting and may contain minor changes with respect to the published edition.

The present version is accessible on PORTO, the Open Access Repository of the Politecnico of Torino, in compliance with the publisher's copyright policy.

Copyright owner: *Elsevier*.

¹Dipartimento di Scienza dei Materiali ed Ingegneria Chimica, Politecnico di Torino, Corso

Duca degli Abruzzi 24, 10129 Torino, Italy, email: gebavi@yahoo.com

²Departamento de Física Aplicada I, Escuela Superior de Ingenieros, Alda. Urquijo s/n 48013

Bilbao, Spain and Center of Materials Physics CSIC-UPV/EHU and Donostia International

Physics Center, Apartado 1072, 20080 San Sebastian, Spain

³Swansea University, Singleton Park, School of Engineering, Multidisciplinary

Nanotechnology Centre, Swansea SA2 8PP, UK

Keywords: tellurite glass, thulium, holmium, energy transfer

Abstract

In this study, thermal and spectroscopic properties of Tm^{3+} and Ho^{3+} codoped tellurite glasses over a wide dopant concentration range are reported in order to assess their potential laser performance under 790 nm diode laser excitation and to identify specific candidates for fiber laser operation. Energy transfer microparameters and critical ion distances are determined for ${}^3\text{H}_4$, ${}^3\text{F}_4$ (Tm^{3+}) and ${}^5\text{I}_7$ (Ho^{3+}) emission levels in the framework of diffusion – limited regime and dipole – dipole interaction.

1. Introduction

There is currently great interest in emission and interaction features of the rare earth (RE) ions such as Er^{3+} , Nd^{3+} , Pr^{3+} , Ho^{3+} , Tm^{3+} , and Yb^{3+} in order to develop fiber lasers emitting in near infrared region (NIR). As a matter of fact, holmium (Ho^{3+}) emission from the first excited level ${}^5\text{I}_7 \rightarrow {}^5\text{I}_8$ lies in the 1.95 to 2.15 μm wavelength range which offers numerous applications in medicine, range monitoring, and sensing [1, 2]. However, direct pumping of this transition is not obtainable by commercial diode lasers, and therefore alternative ways such as pumping with Tm^{3+} doped fiber laser or sensitizing with Tm^{3+} are utilized. Considering the second case, $\text{Tm}^{3+} - \text{Ho}^{3+}$ doped system, where the pump photon at ~ 790 nm excites Tm^{3+} to ${}^3\text{H}_4$ level offers highly efficient energy transfer (ET) to an activator ion and numerous transition processes.

The cross – relaxation (CR: ${}^3\text{H}_4, {}^3\text{H}_6 \rightarrow {}^3\text{F}_4, {}^3\text{F}_4$) process contributes to the population of ${}^3\text{F}_4$ level from where quasi resonant ET to neighboring Ho^{3+} occurs followed by the ${}^5\text{I}_7 \rightarrow {}^5\text{I}_8$ transition and corresponding emission at ~ 2050 nm (Fig. 1).

The challenge of building $\text{Tm}^{3+} - \text{Ho}^{3+}$ doped fiber laser is to ensure an adequate population inversion, to avoid ETU from upper laser level, and to reduce back energy transfer processes. Regarding such aims, the choice of the host material, sensitizer and activator ion concentration, as well as pumping characteristics should be optimized.

Several articles related to $\text{Tm}^{3+} - \text{Ho}^{3+}$ fiber lasers based on silica or tellurite glass hosts are published in the last years. Emission at 2.1 μm in water cooled $\text{Tm}^{3+} - \text{Ho}^{3+}$ doped silica fiber system with 83 W pump power was demonstrated [3]. High energy pulse laser (1.1 J/pulse at 2 Hz rep. rate and 187 ns pulse duration) in $\text{Tm}^{3+} - \text{Ho}^{3+}$ system pumped with commercial diode laser and emission at 2.053 μm was reported as well [4].

Regarding tellurite glasses, CW and Q-switched $\text{Tm}^{3+} - \text{Ho}^{3+}$ fiber laser in $80\text{TeO}_2 - 10\text{ZnO} - 10\text{Na}_2\text{O}$ (mol %) host composition was demonstrated in 2008 [5]. Pumping was carried out by using an $\text{Yb}^{3+}/\text{Er}^{3+}$ doped silica fiber laser at 1.6 μm and a pumping efficiency of 62% (for CW) and a 0.1 W threshold were obtained. However, this efficiency does not take into account the $\text{Yb}^{3+}/\text{Er}^{3+}$ laser efficiency (reasonably $< 50\%$) and therefore we expect that direct diode pumping of Tm^{3+} will provide significantly better results.

As evident from the literature overview, the choice of the active material is critical for various spectroscopic parameters. The reasons for choosing a tellurite glass host are its high RE solubility, low phonon energy, high refractive index, and thermal stability [6]. Our previous work [7] reported highly Tm^{3+} doped tellurite glasses specifying the optimal dopant concentration region for short cavity fiber laser. This study extends the previous work by shifting the emission towards longer wavelengths with introducing Ho^{3+} in the same tellurite based, glass host.

The major task of this paper is to investigate Tm^{3+} and Ho^{3+} energy transfer in a low and high dopant region by utilizing steady-state and time-resolved laser spectroscopy. The energy transfer microparameters and critical ion distances have been determined for ${}^3\text{H}_4$, ${}^3\text{F}_4$

(Tm³⁺) and ⁵I₇ (Ho³⁺) emission levels in the framework of diffusion – limited regime and dipole – dipole interaction.

2. Experimental techniques

2.1. Glass fabrication

Glasses were prepared by melt quenching from mix powder batches, inside a glove box in a dry atmosphere with water content of about 7 ppm. The chemicals employed (together with their purity) were the following: TeO₂ (99+%), ZnO (99.99%), Na₂CO₃ (99.995%), Tm₂O₃ (99.99%), Ho₂O₃ (99.9%). Relative molar ratio of the host glass constituent oxides was kept the same for all samples, regardless of Tm³⁺ and Ho³⁺ doping. The fabricated samples were based on the host composition 75TeO₂:20ZnO:5Na₂O (mol%) doped with increasing amounts of Tm³⁺ and Ho³⁺. Glass melting was carried out in a Pt crucible at around 900 °C for 4h, then pouring on a preheated brass plate at 300 °C and annealing followed. The whole process required around 30 h of operation.

2.2 Glass characterization: thermo – mechanical properties

Thermal analysis was performed on fabricated glasses using a Perkin Elmer DSC-7 differential scanning calorimeter up to 550°C under Ar flow with a heat rate of 10°C/min in Al pans using 30 mg glass samples. Thermal analysis was employed to determine the effect of glass composition on glass stability which can be measured with the quantity T_x-T_g (T_x is crystallization peak onset value and T_g is glass transition temperature).

2.3 Glass characterization: optical properties

Refractive index was measured for all samples at five different wavelengths (533, 825, 1061, 1312 and 1533 nm) by the prism coupling technique (Metricon, model 2010). The

instrument resolution was ± 0.0001 . Five scans were used for each measurement. Standard deviation in refractive index at different points of the same sample was around ± 0.0003 .

The steady-state emission measurements were made with a Ti-sapphire ring laser (0.4 cm^{-1} linewidth) at 793 nm of excitation wavelength. The fluorescence was analyzed with a 0.25 monochromator, and the signal was detected by a PbS detector and finally amplified by a standard lock-in technique. For the fluorescence dynamic measurements of the IR emission of Ho^{3+} a digital oscilloscope was used to record the decay signal. Lifetime measurements for Tm^{3+} ions were obtained by exciting the samples with a Ti-sapphire laser pumped by a pulsed frequency doubled Nd:YAG laser (9 ns pulse width), and detecting the emission with a Hamamatsu R5509-72 photomultiplier. Data were processed by a Tektronix oscilloscope. All measurements were performed at room temperature.

3. Experimental results and discussion

3.1 Samples overview, DSC analysis and refractive index values

Glasses were named by using the following scheme: “T” stands for Tm whilst “H” for Ho both followed by a number indicating the mol% content of dopant ions in the prepared glass. Table 1 shows the list of glasses prepared for this study together with their dopant concentrations, thermal properties and refractive index values. In the ‘Group I’, concentration of Tm^{3+} ions was constant, whereas the Ho^{3+} concentration was ranging from 0 to 3 mol%. Similar nomenclature was used for glasses in group II and III.

Tab. 1 shows that glass stability ΔT increases with the addition of Ho^{3+} for low concentrations (Group I), up to the sample T4H5 (Group II) where ΔT starts to decrease with Ho^{3+} addition. Glass stability progressively decreases in Group III as well. Two crystallization peaks were observed for highly doped glasses in Groups II and III.

The refractive index values are shown to decrease with increasing Tm^{3+} or Ho^{3+} concentration and wavelength.

3.2 Emission spectra of Tm^{3+} - Ho^{3+} doped TZN glasses

Figures 2 a, b show, as an example, the emission spectra of Tm^{3+} - Ho^{3+} doped glasses, group I and group II, respectively obtained under excitation at 793 nm in the $^3\text{H}_4$ (Tm^{3+}) level. There are three characteristic regions which have origin at the emission of thulium $^3\text{H}_4$ and $^3\text{F}_4$ levels or holmium $^5\text{I}_7$ level. Holmium $^5\text{I}_7$ level shows as the double peak with two characteristic emissions: at shorter wavelengths in the range from 1970 – 2045 nm (signed as ‘A’) and at longer wavelengths in the range from 2024 – 2080 nm (signed as ‘B’).

As can be seen in these figures, the emission intensity of the $^3\text{F}_4 \rightarrow ^3\text{H}_6$ transition decreases in the codoped samples as Ho^{3+} concentration increases due to the energy transfer from Tm^{3+} ($^3\text{F}_4$) to Ho^{3+} ($^5\text{I}_7$). In group II glasses system, the Ho^{3+} emission around 2 μm decreases for Ho^{3+} concentrations higher than 2 mol% Ho^{3+} due to concentration quenching.

Fig. 3a shows the absorption and emission cross-sections corresponding to the $^5\text{I}_7 \leftrightarrow ^5\text{I}_8$ transitions of Ho^{3+} . The absorption cross section has been calculated by using the expression: $\sigma_{\text{abs.}}(\lambda) = \alpha(\lambda)/N$, where $\alpha(\lambda)$ is the experimental absorption coefficient and ‘N’ is the concentration of Ho^{3+} ions. The emission cross-section shown in Fig. 3a has been obtained by the McCumber theory [8]:

$$\sigma_{\text{emiss.}} = \sigma_{\text{abs.}} \cdot \frac{Z_L}{Z_U} \cdot \exp \left[\frac{hc}{k_B T} \left(\frac{1}{\lambda_{ZL}} - \frac{1}{\lambda} \right) \right] \quad (1)$$

where Z_U , Z_L , λ , k_B , and E_{ZL} denote the partition functions of the upper and lower states, transition wavelengths, Boltzmann’s constant, and the so – called ‘zero line’ energy,

respectively [9]. The partition function ratio and zero line energy used for ${}^5I_8 \rightarrow {}^5I_7$ were, $Z_L/Z_U = 0.81$, and $\lambda_{ZL} = 5153 \text{ cm}^{-1}$ (1941 nm) [10].

Under assumption that the electrons in Ho^{3+} are either in state 5I_7 or 5I_8 , the gain coefficient $G(\lambda)$ can be written as: $G(\lambda) = N (p\sigma_{em} - (1-p)\sigma_{abs})$ where N is the number of Ho^{3+} ions, ‘ p ’ is the population inversion rate, and σ_{em} and σ_{abs} are emission and absorption cross sections, respectively [11].

Figure 3b shows the effective cross section (G/N) as a function of wavelength obtained for different values of ‘ p ’. When population inversion decreases ($0.6 < p < 0.99$), the gain peak at shorter wavelengths ‘A’ decreases whilst the ‘B’ peak shifts to longer wavelengths, becomes broader and lower in intensity. Furthermore, a net gain suitable for laser action is achieved at longer wavelength when about 40% Ho^{3+} are in excited state. Note that for $p = 0.4$ an effective cross section of 10^{-21} cm^2 is achieved. This corresponds to a single-pass gain of 1.9 dB over only 2 cm for glass with Ho^{3+} doping of 1 mol% (about 2.2×10^{20} ions/cm³). This value shows that Ho^{3+} doping concentration of 1 mol% is suitable for ultracompact laser.

The same behavior of ‘A’ and ‘B’ peaks is observed in the experimental results (Fig. 2b). As the Ho^{3+} content increases, 3H_4 and 3F_4 levels are quickly depleted due to cross – relaxation and energy transfer to Ho^{3+} , respectively. Besides that, Ho^{3+} emission at longer wavelengths (signed as ‘B’) increases in intensity whilst the one at shorter wavelengths (signed as ‘A’) decreases.

As already observed in the single Tm^{3+} doped TZN composition [7], the increase of Tm^{3+} content reduces the emission from 3H_4 level which can also be observed in the case of Tm^{3+} - Ho^{3+} doping, but with increased depopulation rate.

3.3 Fluorescence lifetimes of level ${}^3\text{H}_4$

The lifetimes of level ${}^3\text{H}_4$ (Group I) were calculated from the decay curves obtained by exciting at 793 nm and collecting the luminescence at 1475 nm. The decays show nonlinear time dependence in a semilogarithmic scale for all monitored samples (Fig. 4).

The decay curves show that the ${}^3\text{H}_4$ lifetimes of Tm^{3+} are reduced in the presence of Ho^{3+} for the same sensitizer concentration. This effect has been previously observed in tellurite glasses and attributed to the $\text{Tm}^{3+}:{}^3\text{H}_4 \rightarrow \text{Ho}^{3+}:{}^5\text{I}_7$ energy transfer [12]. In this process Tm^{3+} ions are transferred from ${}^3\text{H}_4$ to ${}^3\text{H}_5$, and then relax to ${}^3\text{F}_4$ through multiphonon relaxation. Tm^{3+} ions in the ${}^3\text{F}_4$ state transfer their energy to ${}^5\text{I}_7$ (Ho^{3+}) state.

The average lifetime values reported in Table 2 are calculated by utilizing the expression [13]: $\langle \tau \rangle = \frac{\int I(t)dt}{I(t=0)}$.

Quantum efficiency $\eta = \tau_{SA}/\tau_0$, of the ${}^3\text{H}_4$ level decreases with the increase of Ho^{3+} content. Radiative lifetime of ${}^3\text{H}_4$ level is taken as 347 μs from the previous study [7].

Energy transfer probability (W) and ET efficiency (η^d) can be calculated by measuring the sensitizer lifetime with (τ_{SA}) and without (τ_S) activators presence. Their values increase with Ho^{3+} concentration. In the heavily doped glasses sensitizer ions are closer to the activator, and therefore the ET is more probable. Energy transfer parameter 'K' slightly decreases its value with increasing activator concentration.

In the case of groups II and III, the emission from level ${}^3\text{H}_4$ is practically quenched due to cross-relaxation processes.

The sensitizer fluorescence decays in the single doped samples showed the existence of energy migration among Tm^{3+} ions [7] which can be described by the diffusion or hopping

model. The best agreement between experimental data and theoretical fit is obtained with the expression corresponding to the Yokota-Tanimoto model in the case of dipole-dipole interaction [18]:

$$\phi(t) = \phi(0) \cdot e^{-t/\tau_0} \cdot \exp \left[-\frac{4}{3} \cdot \pi^{3/2} \cdot N_A \cdot (C_{SA} \cdot t)^{1/2} \cdot \left(\frac{1 + 10.87x + 15.5x^2}{1 + 8.743x} \right)^{3/4} \right] \quad (2)$$

where τ_0 is radiative lifetime, N_A is the acceptor concentration, $x = 0.5 \left(\frac{4\pi}{3} \right)^{4/3} C_{SS} C_{SA}^{-1/3} N^{4/3} t^{2/3}$, C_{SA} and C_{SS} are ET microparameters for SA and SS interactions respectively. For the calculations, the following parameterization can be used: $A = \frac{4}{3} \pi^{3/2} N_A C_{SA}^{1/2}$, $B = 0.5 \left(\frac{4\pi}{3} \right)^{4/3} C_{SS} C_{SA}^{-1/3} N^{4/3}$. Value of parameter 'B' can be also expressed as $B = DC^{-1/3}$ with 'D' as a diffusion coefficient [17].

The obtained values for parameters A and B, energy transfer microparameter C_{SA} , and diffusion coefficient are displayed in Tab. 3 for the samples of group I. This table also shows the values for the critical radius R_0 , which is defined as the distance at which the probability of the energy transfer process becomes equal to the intrinsic decay rate of the metastable level and can be calculated in terms of C_{SA} and τ_R from $R_0^6 = \tau_R C_{SA}$.

The ET microparameter C_{SA} increases as Ho^{3+} concentration increases. Parameters taken from Tab. 3 and Tab. 4 can be inserted into the equations suggested in literature [18]: $K_D = 1/\tau_{SA} - 1/\tau_0$ also defined by $K_D \sim 4\pi D N_A (C_{SA}/D)^{1/4}$ (where N_A is activator concentration), respectively. Comparison shows the same order of magnitude for K_D obtained from lifetime measurements and Yokota – Tanimoto fit for all three samples.

3.4 Fluorescence of levels 3F_4 and 5I_7

The lifetimes of levels 3F_4 and 5I_7 were calculated from the decay curves obtained under excitation at 793 nm and by collecting the luminescence at 1680 nm and 2050 nm, respectively.

The decays can be described by a single exponential function to a good approximation for all samples (Fig. 4, 5).

Table 4 shows the lifetime values obtained by fitting the experimental decays to a single exponential function together with the corresponding quantum efficiencies.

Radiative lifetime values can be calculated from equation:

$$\frac{1}{\tau_{rad}} = 8 \cdot \pi \cdot n^2 \cdot c \cdot \frac{g_{lower}}{g_{upper}} \int \frac{\sigma_{abs}(\lambda)}{\lambda^4} d\lambda \quad [19]$$

without including any uncertainty of J-O parameters. The value obtained for the ${}^5I_7 \rightarrow {}^5I_8$ transition was $\tau_0({}^5I_7) = 6.57$ ms

Groups II and III include highly sensitized glasses where S-S diffusion is much faster than S-A transfer rate. Consequently, excitations among Tm^{3+} spread very quickly, creating a uniform local distribution in excited manifolds [20].

As shown in Tab. 4, whereas the lifetimes of level 3F_4 in the single doped samples decrease as Tm^{3+} concentration increases, these lifetimes are approximately the same as those of level 5I_7 in the codoped glasses. The expected shortening of the 3F_4 lifetime in the codoped samples, due to the additional probability for relaxation by nonradiative energy transfer to Ho^{3+} ions, is not observed in these glasses which indicate that the energy transfer between ions is very fast compared with their upper state lifetimes and the two excited states are in quasi-thermal equilibrium. In this case, it is not possible to evaluate the energy transfer efficiency from Tm^{3+} (3F_4) to Ho^{3+} (5I_7) ions by using the lifetime values of Tm^{3+} in the single

and codoped samples. A similar behaviour was found by Zou and Toratani in fluoride glasses [21].

3.5 Fluorescence characteristics of compared samples

In the subsection 3.2, McCumber theory has been used for Ho³⁺ ions emission cross section calculation. In the present subsection, the alternative Fuchtbauer – Ladenburg (FL) equation will be used for calculating Tm³⁺ and Ho³⁺ emission cross section: $\sigma_e = \lambda_p^4 \beta / (8\pi n^2 c \tau_0 \Delta\lambda_{eff.})$, where λ_p is the peak fluorescence wavelength, β is the branching ratio, n the refractive index, c is the light velocity, τ_0 is the radiative lifetime and $\Delta\lambda_{eff.}$ is the effective linewidth calculated by using the relation: $\Delta\lambda_{eff.} = \int I(\lambda) / I_{max} d\lambda$ [21, 22, 23].

The probability of energy transfer between sensitizer ('S', Tm³⁺) and activator ('A', Ho³⁺) depends on the spectral overlapping between 'S' emission and 'A' absorption [24]. The increase of S or A concentration will decrease mutual distance, which changes the ET rate [25], enhances the Ho³⁺ ↔ Tm³⁺ back-transfer and enables energy diffusion among S or A ions.

To evaluate the extent of each energy transfer we have calculated the critical radii from the spectral overlap between the emission cross-section of sensitizers and absorption cross-section of activators [26]:

$$R_{SS}^6 = \frac{6c\tau_s}{(2\pi)^4 \cdot n^2} \cdot \frac{g_s^{low}}{g_s^{up}} \cdot \int \sigma_{emiss.}^S \cdot \sigma_{abs.}^S d\lambda \quad (3a)$$

$$R_{SA}^6 = \frac{6c\tau_s}{(2\pi)^4 \cdot n^2} \cdot \frac{g_s^{low}}{g_s^{up}} \cdot \int \sigma_{emiss.}^S \cdot \sigma_{abs.}^A d\lambda \quad (3b)$$

$$R_{AS}^6 = \frac{6c\tau_s}{(2\pi)^4 \cdot n^2} \cdot \frac{g_A^{low}}{g_A^{up}} \cdot \int \sigma_{emiss.}^A \cdot \sigma_{abs.}^S d\lambda \quad (3c)$$

where ‘ g_A ’ or ‘ g_S ’ is the degeneracy of acceptor or sensitizer, respectively; ‘ n ’ is the refractive index, and ‘ c ’ is the light speed.

Absorption and emission cross-sections of sample T1H3 used to evaluate the overlapping integral are shown on Fig. 6 a, b, c. McCumber calculations for Tm^{3+} and Ho^{3+} ions are used following the literature [10, 27] together with FL equation.

Discrepancy between McCumber and FL comes from error in λ_{ZL} and τ_0 determination. Radiative lifetime can be over-estimated because of self - trapping or under-estimated due to nonradiative processes.

The values of the $Tm^{3+}(^3F_4) \rightarrow Tm^{3+}(^3F_4)$, $Tm^{3+}(^3F_4) \rightarrow Ho^{3+}(^5I_7)$, and $Ho^{3+}(^5I_7) \rightarrow Tm^{3+}(^3F_4)$, energy transfer microparameters are displayed in Tab. 5 for samples T1H3 and T5H4.

Reported ET microparameters in $TeO_2-ZnO-Li_2O-Bi_2O_3-CsCl$ (TZLBC) host [26] are: $1.821 \cdot 10^{-50}$ (m^6/s) ($Tm^{3+} - Tm^{3+}$), $1.872 \cdot 10^{-52}$ (m^6/s) ($Tm^{3+} - Ho^{3+}$), $6.473 \cdot 10^{-54}$ (m^6/s) ($Ho^{3+} - Tm^{3+}$). A review of T1H3 and T5H4 spectroscopic characteristics is given in Tab. 6.

The absorption and emission cross sections of Ho^{3+} in these glasses are higher than those reported by Zou and Toratani in fluorozirconaluminate glasses [21] but lower than in oxyfluoride tellurite glass [28].

As can be seen in Tab. 6, the laser parameter $\sigma_{\text{emiss}}\tau$ is higher for the T1H3 glass which indicates that activator emission could be maximized by keeping the thulium content lower than holmium.

The ET microparameters ratio shows that forward energy transfer is much faster than backward and only 2-3% of thulium ions are settled at level 3F_4 due to back – energy transfer.

4. Conclusions

This work reports thermal and spectroscopic properties of low and highly Ho^{3+} -doped tellurite glasses sensitized with Tm^{3+} .

Obtained values of the radiative lifetimes of levels 3F_4 (Tm^{3+}) and 5I_7 (Ho^{3+}) are 2.06 and 6.57 ms, respectively. The longest Ho^{3+} fluorescence lifetime of 5.58 ms corresponds to a Ho^{3+} concentration of $1.6 \cdot 10^{20} \text{ cm}^{-3}$. Decrease of Ho^{3+} lifetime by S or A concentration increase is observed for all glass groups.

Fluorescence spectroscopy showed strong depletion of thulium 3H_4 and 3F_4 levels in the presence of Ho^{3+} ions which indicates high efficient energy transfer towards activator ions. The Ho^{3+} emission from level 5I_7 shifts to longer wavelengths and its intensity decreases as Ho^{3+} content increases.

The fluorescence decays of level 3H_4 can be described by a dipole-dipole energy transfer process assisted by energy migration. The energy transfer microparameters and critical radius increase with increasing Ho^{3+} content.

Energy transfer microparameters regarding level 3F_4 are calculated by using the integral overlap of S-A spectra. Obtained values are $1.17 \cdot 10^{-50} \text{ m}^6\text{s}^{-1}$ ($\text{Tm}^{3+} \rightarrow \text{Tm}^{3+}$), $5.65 \cdot 10^{-51} \text{ m}^6\text{s}^{-1}$ ($\text{Tm}^{3+} \rightarrow \text{Ho}^{3+}$), and $1.15 \cdot 10^{-52} \text{ m}^6\text{s}^{-1}$ ($\text{Ho}^{3+} \rightarrow \text{Tm}^{3+}$). Parameter $\sigma_{\text{emiss}}\tau(\text{Ho}^{3+})$ showed great advantages of T1H3 vs. T5H4 glasses.

In order to obtain optimum energy storage of the lasing ion, low activator and high sensitizer glasses should be considered. Quantum efficiency drops abruptly with activator concentration increase. Moreover, attention should be paid to reabsorption and upconversion processes which may occur for high activator concentrations in optical fiber geometry, and thus increase laser threshold.

Acknowledgments

The authors wish to thank the Regione Piemonte Converging Technologies “Hipernano” research project. R. Balda and J. Fernández acknowledge financial support from the Spanish Ministry of Science and Innovation under project MAT2009-14282-C02-02 and from the Basque Country Government (IT-331-07).

References

- [1] B.M. Walsh, *Laser Physics* 19 (4) (2009) 855-866.
- [2] Mark E. Storm, *IEEE J. of Quant. Elect.* 29 (2) (1993) 440-451.
- [3] D.G. Lancaster, A. Sabella, A. Hemming, S. Bennetts, S.D. Jackson, *The Optical Society of America, Technical Digest, Washington, 2007.*
- [4] J. Yu, B.C. Trieu, E.A. Modlin, U.N. Singh, M.J. Kavaya, S. Chen, Y. Bai, P.J. Petzar, M. Petros, *Opt. Lett.* 31 (2006) 462–464.

- [5] Y. Tsang, B. Richards, D. Binks, J. Lousteau, A. Jha, *Opt. Letters* 33 (11) (2008) 1282–1284.
- [6] H. Gebavi, D. Milanese, G. Liao, Q. Chen, M. Ferraris, M. Ivanda, O. Gamulin, S. Taccheo, *J. Non. Cryst. Solids* 355 (9) (2009) 548 – 555.
- [7] *J. Phys. D: Appl. Phys.* 43 (2010) 135104
- [8] D.E. McCumber, *Phy. Review* 136 (4A) (1964) 954 - 957.
- [9] X. Zou, H. Toratani, *J. Non. Cryst. Solids* 195 (1996) 113-124.
- [10] S. A. Payne, L. L. Chase, Larry K. Smith, Wayne L. Kway, William F. Krupke, *IEEE J. Quant. Electronics* 28 (1) (1992) 2619 - 2630.
- [11] G. X. Chen, Q. Y. Zhang, G. F. Yang, Z. H. Jiang, *J. Fluoresc.* 17 (2007) 301–307.
- [12] S. Shen, A. Jha, E. Zhang, S.J. Wilson, *C.R. Chimie* 5 (2002) 921-938.
- [13] D. F. de Sousa, R. Lebullenger, A. C. Hernandez, L. A. O. Nunes, *Phy. Rev. B*, 65, (2002) 94294.
- [14] A. Braud, Sylvain Girard, J. L. Doualan, R. Moncorge, *IEEE J. of Quant. Elect.* 34 (11) (1998) 2246–2255.

- [15] R. Lisiecki, W. Ryba-Romanowski, T. Łukasiewicz, *Appl. Phys. B* 83 (2006) 255–259.
- [16] S. Shen, A. Jha, E. Zhang, S. Wilson, *J. Lumin.* 126 (2007) 434–440.
- [17] R. Balda, J. Fernandez, M. A. Arriandiaga, L.M. Lacha, J.M. Fernandez-Navarro, *Opt. Materials* 28 (2006) 1253-1257.
- [18] A. Brenier, C. Pedrini, B. Moine, J.L. Adam, C. Pledel, *Phy. Review B* 41 (8) (1990) 5364.
- [19] Digonnet, Michael J. F, *Rare Earth Doped Fiber Lasers and Amplifiers Optical Engineering*, CRC Press, 1993.
- [20] B. M. Walsh, N. P. Barnes, B. Di Bartolo, *J. Lumin.* 75 (1997) 89-98.
- [21] X. Zou, H. Toratani, *J. Non. Cryst. Solids* 195 (1996) 113-124.
- [22] R. Balda, L.M. Lacha, J. Fernandez, M. A. Arriandiaga, J.M. Fernandez-Navarro, D. Munoz-Martin, *Opt. Express* 16 (16) 2008) 11836.
- [23] L. Qiongfai, X. Haiping, Z. Yuepin, W. Jinhao, Z. Jianli, H. Sailong, *J. Rare Earths* 27 (1) (2009) 76.
- [24] F. Auzel, *Chem. Rev.* 104 (2004) 139-173.

[25] B. M. Walsh, N. P. Barnes, B. Di Bartolo, *J. Lumin.* 90 (2000) 39-48.

[26] L.D. da Vila, L. Gomes, C.R. Eyzaguirre, E. Rodriguez, C.L. Cesar, L.C. Barbosa, *Opt. Materials* 27 (2005) 1333–1339.

[27] X. Haiping, L. Qiongfei, Z. Jianli, Z. Qinyuan, *J. Rare Earths* 27 (5) (2009) 781.

[28] G. Gao, G.Wang, C. Yu, J. Zhang, L. Hu, *J. Lumin.* 129 (2009) 1042–1047.

Tables

Table 1. Tm³⁺-Ho³⁺ doped tellurite glasses prepared for the present study: Tm³⁺ and Ho³⁺ ion content in cm⁻³, glass transition (T_g), crystallization temperature (T_x) and refractive index values are reported. The experimental error for T_g and T_x is ±3 °C.

Group	Sample name	Tm ³⁺	Ho ³⁺	T _g	T _x -T _g	n
		10 ²⁰ (cm ⁻³)	10 ²⁰ (cm ⁻³)	(°C)	(°C)	(1533 nm)
I	T1H0	2.28	-	313	134	1.9918
	T1H0.7	2.28	1.6	315	139	1.9882
	T1H1	2.3	2.8	316	147	1.9860
	T1H3	2.26	6.79	325	167	1.9822
II	T4H0	9.06	-	321	152	1.9833
	T4H2	8.92	4.46	329	152	1.9738
	T4H4	8.89	8.89	331	143	1.9654
	T4H5	8.87	11.08	336	117	1.9633
III	T5H0	11.3	-	320	149	1.9792
	T5H2	11.07	4.43	334	141	1.9717
	T5H4	11.06	8.85	340	121	1.9624
	T5H5	11.05	11.05	341	102	1.9605

* T measuring error is ±0.0001

**n deviation throughout the same sample is ±0.0003

Table 2. J-O parameters comparison with literature.

Author	Sample composition	Ω ₂	Ω ₄	Ω ₆
[16]	80TeO ₂ :10ZnO:10Na ₂ O – Tm ³⁺ , Ho ³⁺	5.11	1.17	1.08
[17]	60TeO ₂ :15Na ₂ O:25WO ₃ – Ho ³⁺	5.70	4.0	1.0
[18]	79TeO ₂ : 20Li ₂ CO ₃ – Ho ³⁺	4.98	0.99	2.96
[19]	70TeO ₂ :10ZnO:10ZnF ₂ :2.5Na ₂ O:2.5K ₂ O:5La ₂ O ₃ – Tm ³⁺ , Ho ³⁺	4.20	2.80	1.10
[20]	70TeO ₂ :20WO ₃ :10ZnO – Ho ³⁺	5.26	2.28	2.18
This study	75TeO ₂ :20ZnO:5Na ₂ O – Tm ³⁺ , Ho ³⁺	4.94	2.15	1.62

* Ω [10⁻²⁰ cm²]

Table 3. Transition rates, radiative lifetimes and branching ratios for Tm^{3+} obtained from J – O analysis.

Transition	$\bar{\lambda}$ (nm)	$A_{J'J}$ (s^{-1})	τ_0 (ms)	β
$^1\text{G}_4 \rightarrow ^3\text{H}_6$	480	2952.72		0.51483
$^1\text{G}_4 \rightarrow ^3\text{F}_4$	650	433.68		0.07561
$^1\text{G}_4 \rightarrow ^3\text{H}_5$	790	1638.92	0.17	0.28576
$^1\text{G}_4 \rightarrow ^3\text{H}_4$	1145	577.84		0.10075
$^1\text{G}_4 \rightarrow ^3\text{F}_3$	1478	132.20		0.02305
$^3\text{F}_3 \rightarrow ^3\text{H}_6$	686	5468.30		0.84905
$^3\text{F}_3 \rightarrow ^3\text{F}_4$	1138	155.88	0.16	0.02420
$^3\text{F}_3 \rightarrow ^3\text{H}_5$	1558	808.91		0.12560
$^3\text{F}_3 \rightarrow ^3\text{H}_4$	5552	7.40		0.00115
$^3\text{H}_4 \rightarrow ^3\text{H}_6$	792	3111.05		0.91279
$^3\text{H}_4 \rightarrow ^3\text{F}_4$	1474	242.07	0.29	0.07102
$^3\text{H}_4 \rightarrow ^3\text{H}_5$	2307	55.16		0.01618
$^3\text{H}_5 \rightarrow ^3\text{H}_6$	1225	$13.79_{\text{ED}} + 110.24_{\text{MD}}$	1.47	0.97748
$^3\text{H}_5 \rightarrow ^3\text{F}_4$	4226	649.97		0.02221
$^3\text{F}_4 \rightarrow ^3\text{H}_6$	1820	484.98	2.06	1

Table 4. Transition rates, radiative lifetimes and branching ratios for Ho³⁺ obtained from J – O analysis

Transition	$\bar{\lambda}$ (nm)	$A_{J'J}$ (s ⁻¹)	τ_0 (ms)	β
⁵ F ₄ → ⁵ S ₂	67656	8 10 ⁻⁵		8 10 ⁻⁹
⁵ F ₄ → ⁵ F ₅	3173	21.71		0.00239
⁵ F ₄ → ⁵ I ₄	1887	41.69		0.00460
⁵ F ₄ → ⁵ I ₅	1327	269.79	0.11	0.02974
⁵ F ₄ → ⁵ I ₆	986	535.62		0.05905
⁵ F ₄ → ⁵ I ₇	738	759.92		0.08378
⁵ F ₄ → ⁵ I ₈	536	7441.94		0.82044
⁵ S ₂ → ⁵ F ₅	3330	0.85		1.6 10 ⁻⁴
⁵ S ₂ → ⁵ I ₄	1942	76.03		0.01463
⁵ S ₂ → ⁵ I ₅	1354	79.20	0.19	0.01524
⁵ S ₂ → ⁵ I ₆	1000	324.73		0.06248
⁵ S ₂ → ⁵ I ₇	746	1827.8		0.35168
⁵ S ₂ → ⁵ I ₈	540	2888.80		0.55581
⁵ F ₅ → ⁵ I ₄	4658	0.09		1.9E-5
⁵ F ₅ → ⁵ I ₅	2282	14.68		0.00311
⁵ F ₅ → ⁵ I ₆	1430	188.43	0.21	0.03991
⁵ F ₅ → ⁵ I ₇	961	851.45		0.18033
⁵ F ₅ → ⁵ I ₈	645	3667.00		0.77663
⁵ I ₄ → ⁵ I ₅	4472	12.51		0.06319
⁵ I ₄ → ⁵ I ₆	2064	77.63		0.39197
⁵ I ₄ → ⁵ I ₇	1211	89.06	5.05	0.44970
⁵ I ₄ → ⁵ I ₈	749	18.84		0.09514
⁵ I ₅ → ⁵ I ₆	3831	13.00		0.04426
⁵ I ₅ → ⁵ I ₇	1662	160.06	3.4	0.54483
⁵ I ₅ → ⁵ I ₈	899	120.72		0.41091
⁵ I ₆ → ⁵ I ₇	2934	31.71		0.08960
⁵ I ₆ → ⁵ I ₈	1175	322.17	2.83	0.91040
⁵ I ₇ → ⁵ I ₈	2100	111 _{ED} +41.17 _{MD}	6.57	1

*A_{MD}(⁵I₇) = 41.17 s⁻¹ [16]

Table 5. Lifetime values of level 3H_4 in single and codoped samples, quantum efficiencies (η), transfer rate (W), ET efficiencies and energy transfer parameter (K).

Group	Sample name	$\tau_{SA}(^3H_4)$	$\eta^a)$	$W^b)$	$\eta^c)$	$K^d)$
		(μs)	(%)	$10^3 (s^{-1})$	(%)	(m^6s^{-1})
I	T1H0	147	42.4	0	0	-
	T1H0.7	110	31.7	2.288	25.17	$6.27 \cdot 10^{-50}$
	T1H1	95	27.4	3.724	35.37	$5.78 \cdot 10^{-50}$
	T1H3	62	17.9	9.326	57.8	$6.08 \cdot 10^{-50}$

a) $\eta = \tau_{SA}/\tau_0$, $\tau_0 = 347 \mu s$, efficiency of the 3H_4 level refreezing lifetime of the single ion [27].

τ_{SA} corresponds to the Tm^{3+} lifetime in the presence of Ho^{3+} ions.

b) $W = \frac{1}{\tau_{SA}} - \frac{1}{\tau_S}$, energy transfer (Tm^{3+} - Ho^{3+}) probability [28]

c) $\eta = 1 - \frac{\tau_{SA}}{\tau_S} = W\tau_{SA}$, non - radiative transfer efficiency (Tm^{3+} - Ho^{3+}) [9]

d) $W = \frac{1}{\tau_{SA}} - \frac{1}{\tau_S} = KN_S N_A$, [29]

Table 6. Yokota Tanimoto fit parameters for 3H_4 level of group I.

3H_4 level	A ($s^{-1/2}$)	B ($s^{-2/3}$)	R^2 (%)	C_{SA} $10^{-51} (m^6/s)$	D $10^{-15} (m^2/s)$	R_0 \AA
T1H0	119 \pm 1	92 \pm 3	99.65	4.93	1.57	10.9
T1H0.7	142.8 \pm 0.4	70 \pm 1	99.85	7.13	1.35	11.6
T1H1	160.1 \pm 0.6	104 \pm 2	99.82	8.80	2.15	12
T1H3	224.6 \pm 0.6	134 \pm 2	99.79	17.94	3.51	13.6

* R^2 is the square of the correlation coefficient

Table 7. Lifetime values of 3F_4 and 5I_7 levels and quantum efficiency $\eta(^5I_7)$.

Group	Sample name	$\tau(^3F_4)$	$\tau(^5I_7)$	$\eta(^5I_7)$
		(ms)	(ms)	(%)
I	T1H0	2.42	-	-
	T1H0.7	5.49	5.58	84.93
	T1H1	N.A.	N.A.	-
	T1H3	4.64	4.85	73.82
II	T4H0	0.42	-	-
	T4H2	2.1	2.59	39.42
	T4H4	2.22	2.42	36.83
	T4H5	1.31	1.68	25.57
III	T5H0	0.32	-	-
	T5H2	2.1	1.87	28.46
	T5H4	2.1	1.8	27.40
	T5H5	1.7	1.67	25.42

*used: $\eta = \tau_m/\tau_0$, $\tau_0(Ho^{3+}) = 6.57$ ms

Table 8. Microscopic parameters of the energy transfer processes observed in TZN – Tm³⁺, Ho³⁺ glasses considering dd electric interaction.

Sample	S-A	τ_0 (ms)	R (Å)	C (m ⁶ /s)
T1H3	Tm ³⁺ – Tm ³⁺	3.1	18.2	1.17 10 ⁻⁵⁰
	Tm ³⁺ – Ho ³⁺	3.1	16.1	5.65 10 ⁻⁵¹
	Ho ³⁺ – Tm ³⁺	6.57	9.5	1.15 10 ⁻⁵²
T5H4	Tm ³⁺ – Tm ³⁺	3.1	18.7	1.38 10 ⁻⁵⁰
	Tm ³⁺ – Ho ³⁺	3.1	16.2	5.73 10 ⁻⁵¹
	Ho ³⁺ – Tm ³⁺	6.57	10.4	1.88 10 ⁻⁵²

Table 9. Spectroscopic characteristics of the ⁵I₇→⁵I₈ transition of Ho³⁺ in T1H3 and T5H4 samples.

Parameters	T1H3	T5H4
$\sigma_{\text{abs.}}(\text{Ho}^{3+}) 10^{-25} (\text{m}^2)$	5.90	5.92
$\sigma_{\text{emiss}}(\text{Ho}^{3+}) 10^{-25} (\text{m}^2)$	5.54	5.81
$\tau(\text{Ho}^{3+}) (\text{ms})$	4.85	1.8
$\sigma_{\text{emiss.}}\tau(\text{Ho}^{3+}) 10^{-28} (\text{m}^2 \text{ s})$	26.87	10.46
$C_{\text{AS}}/C_{\text{SA}}$	0.0204	0.0328

Figures

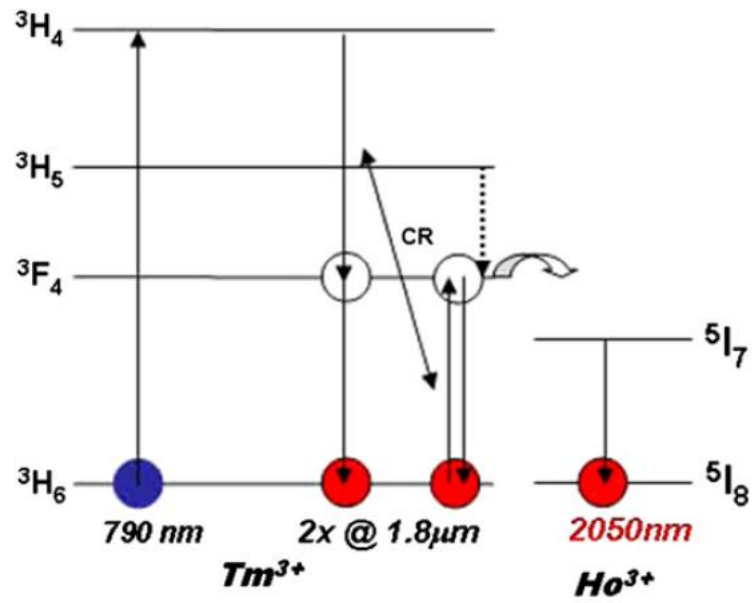


Fig. 1. Tm^{3+} - Ho^{3+} energy levels, cross-relaxation (CR), and $Tm^{3+} \rightarrow Ho^{3+}$ energy transfer for 793 nm pumping scheme; *dashed arrow signs NR processes.

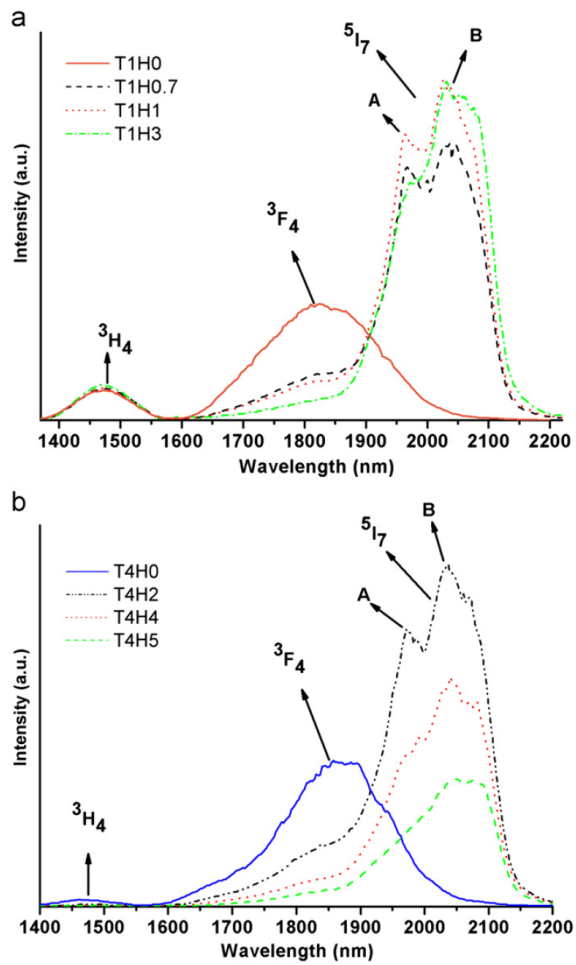


Fig. 2. (a) Emission spectra of Group I. All spectra are normalized on the area under 3H_4 peak. (b) Emission spectra of group II (not normalized).

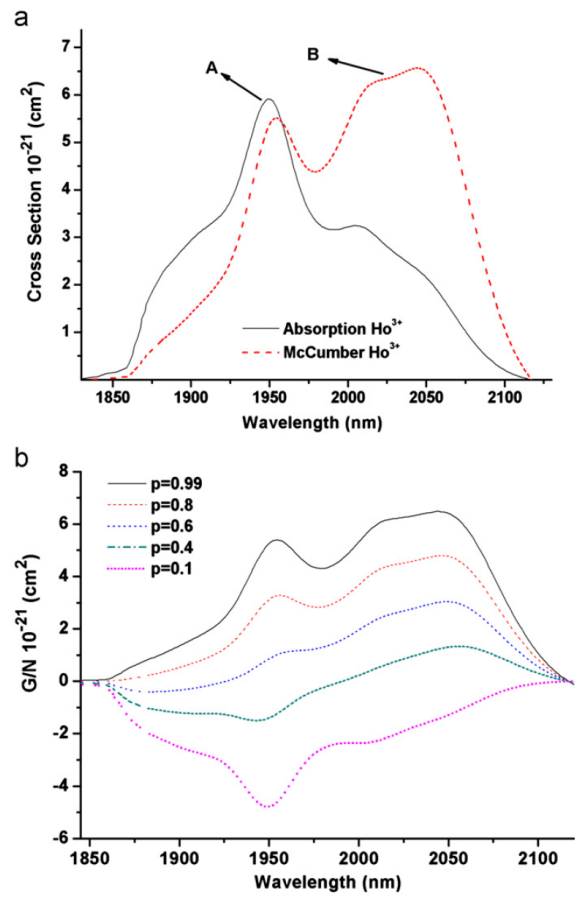


Fig. 3. (a) Absorption and emission cross section for 5I_7 (Ho^{3+}) level (T5H4). (b) Gain coefficient over Ho^{3+} concentration.

wavelengths, becomes broader and lower in intensity. Furthermore, a net gain suitable for laser action is achieved at longer

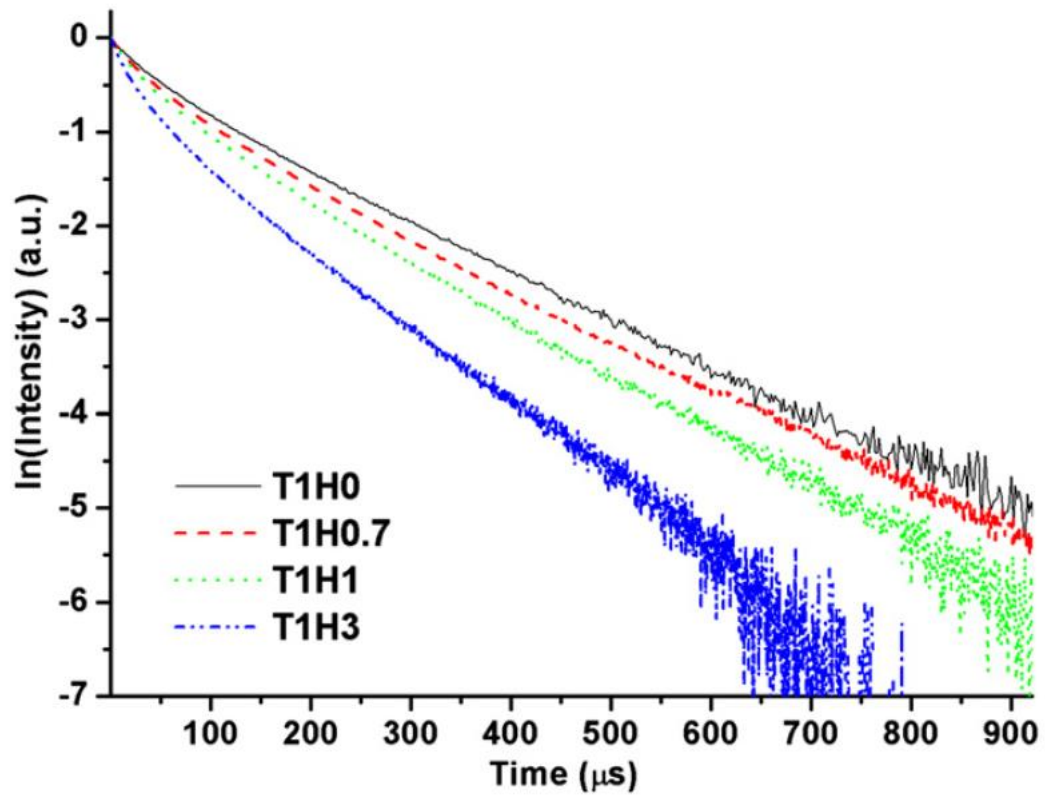


Fig. 4. Decay curves of $^3\text{H}_4$ levels of Group I glasses.

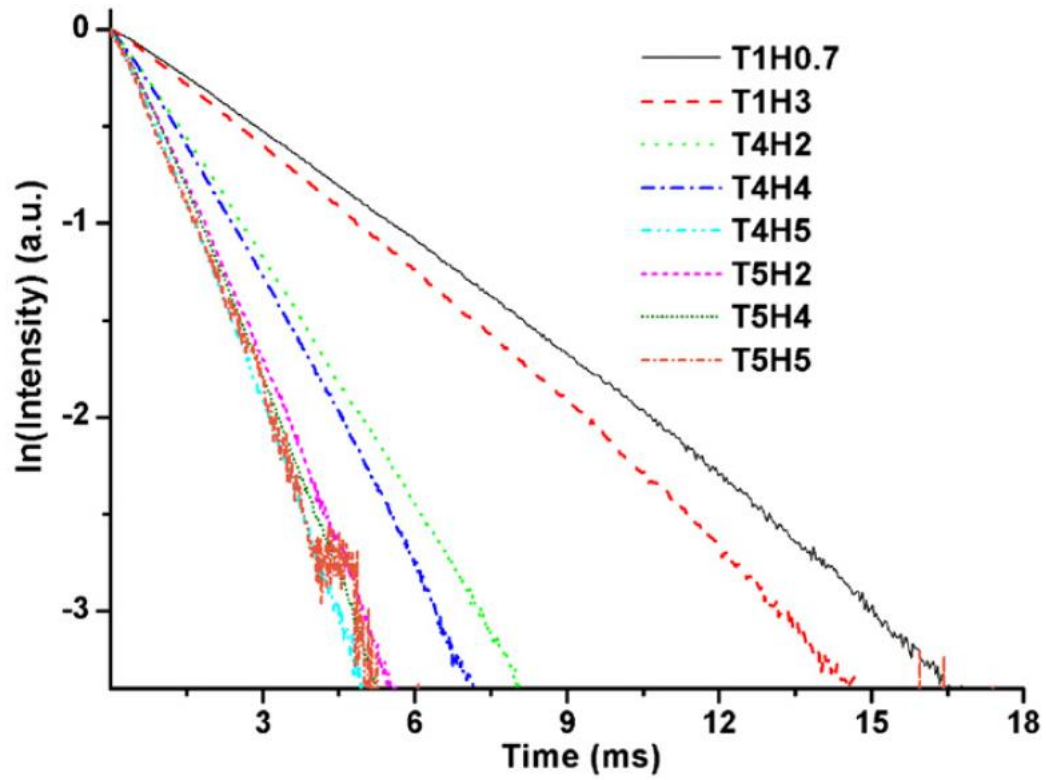


Fig. 5. Decay curves of ${}^5\text{I}_7$ level for all glass groups in semilogarithmic scale.

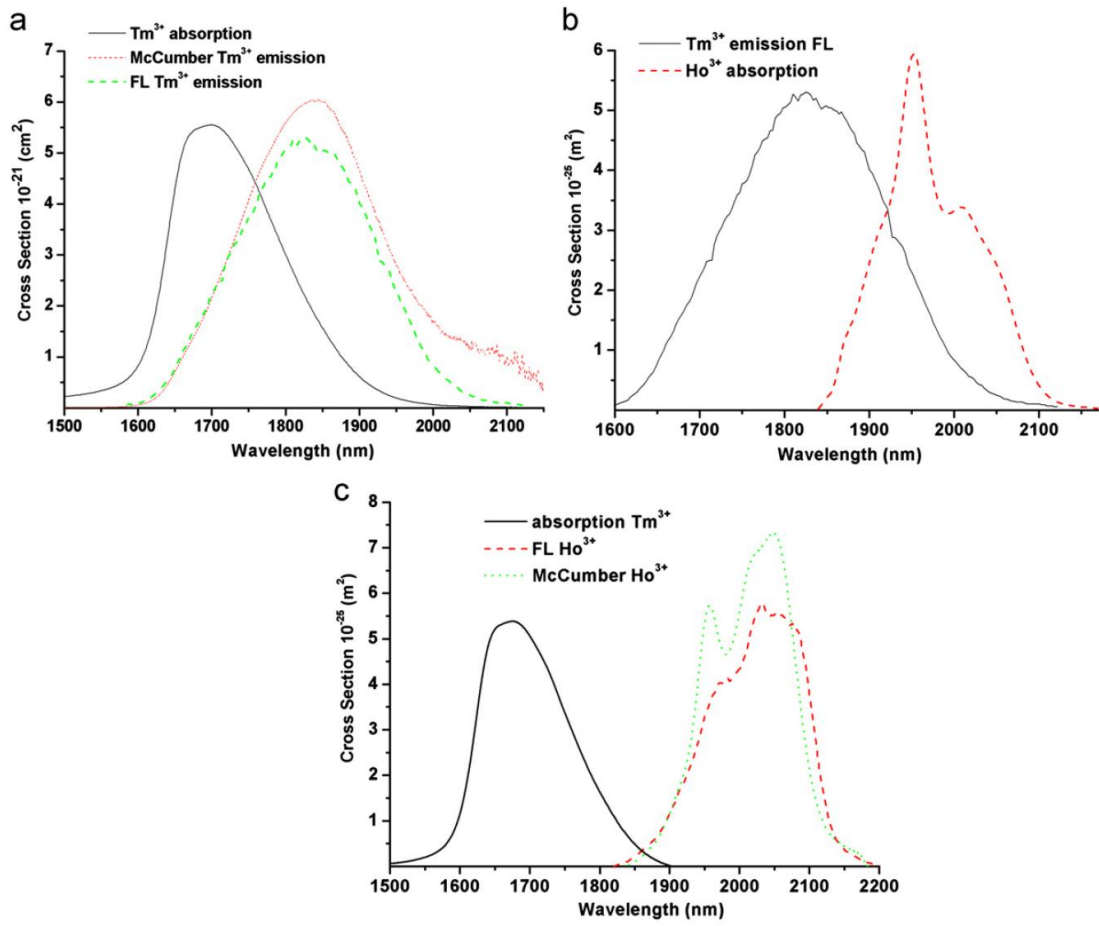


Fig. 6. Overlapping spectra of the T1H3 samples used for evaluation of: (a) Tm³⁺-Tm³⁺ ET, (b) Tm³⁺-Ho³⁺ ET, and (c) Tm³⁺-Ho³⁺ back transfer.